Supplemental Materials

Hydrogel nanoparticle synthesis using liquid-solid separation for more efficient, greener process

Emily N. Ingram, Jason Stallings, Mara Leach, Endras Fadhilah, Anastasia Shaverina, Brittany E. Givens, and Malgorzata Chwatko*

Chemical and Materials Engineering Department, Pigman College of Engineering, University of Kentucky, Lexington, KY

Email: m.chwatko@uky.edu

Methods:

n-Heptane Inverse Emulsion

The oil phase was comprised of 10 ml of n-Heptane, with 0.15M Tween-80 and stirred at 900 rpm in a closed glass vial for 15 minutes prior to the addition of the aqueous phase. Redox polymerization was employed for PEG-DA(575) nanogel synthesis, using 0.75 mM iron gluconate and 0.375mM ammonium persulfate. A 10% w/v emulsion was created by adding 0.5 ml of the PEG-DA(575), iron gluconate, and water layer, simultaneously with 0.5 ml of PEG-DA(575), APS and water layer to n-heptane containing Tween-80. The emulsion stirred for 5 minutes at room temperature at 900 rpm. Two layers had formed following pausing stirring and n-heptane was decanted to isolate the nanogel. Lyophilization was employed to remove the water from the gel and the final recovery of PEG-DA(575) was calculated. Due to Tween-80 use, the nanogels had to be washed with methanol post lyophilization to obtain high purity particles.

Data:

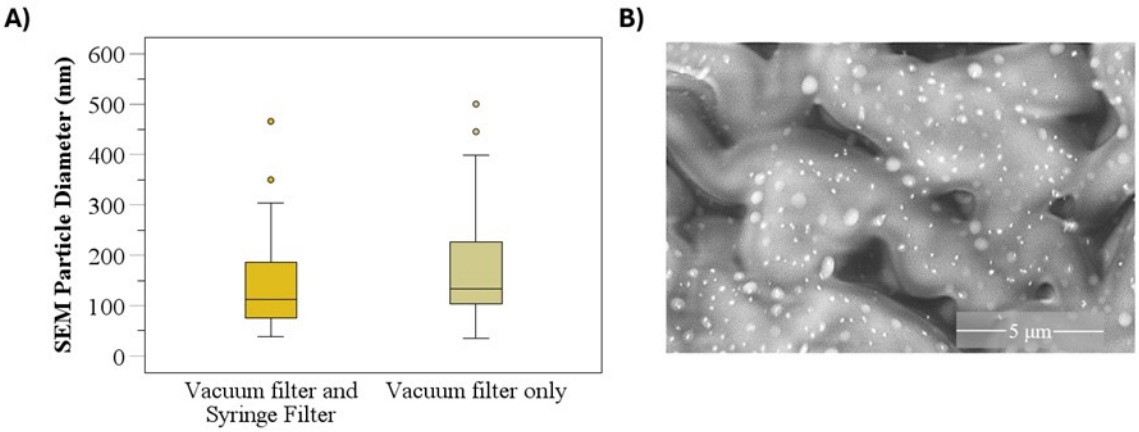

Figure S1. Particle size comparison for PEG-DA(575) nanogels stirring at 900 rpm, using redox polymerization in a nanoemulsion with capric acid as the oil layer. A) Comparison of particle sizes post 2.7 µm vacuum filtration as a single purification method and with a2.7 µm vacuum filtration followed with secondary 1.2 µm syringe filtration. While there is a significant difference t(198) p=0.026, the effect size is small (Cohen's D, 0.386) indicating that syringe filtration does not drastically change the particle size. B) SEM image of PEGDA(575) after vacuum filtration only to observe if there were significant particles lost during the syringe filtration process. The average particle size was 173.6 ± 94.59 nm (n=100, N=2).

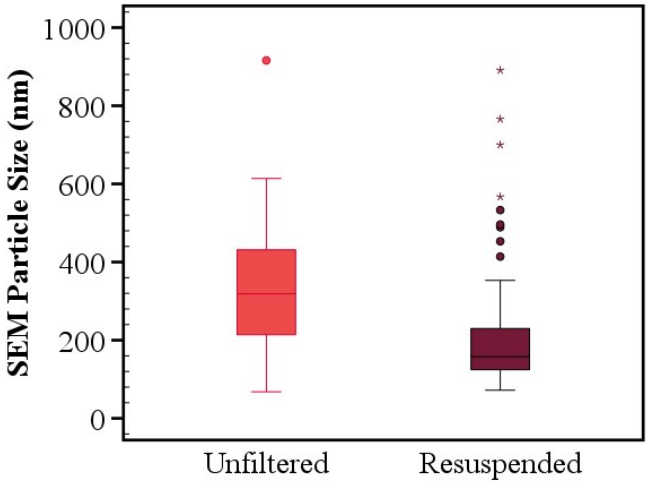

Figure S2. Particle size comparison for PEG-DA(575) nanogels stirring at 100 rpm, using redox polymerization in a nanoemulsion with using and oil to water ratio of 5.4:1, and myristic acid as the oil layer. Comparison of particle sizes directly

after synthesis (n=128, N=2) versus after full purification work up (n=100, N=2). While there is a significant difference t(227) p<0.001, the effect size is large (Cohen's D, 0.869) indicating that syringe filtration does drastically change the particle size.

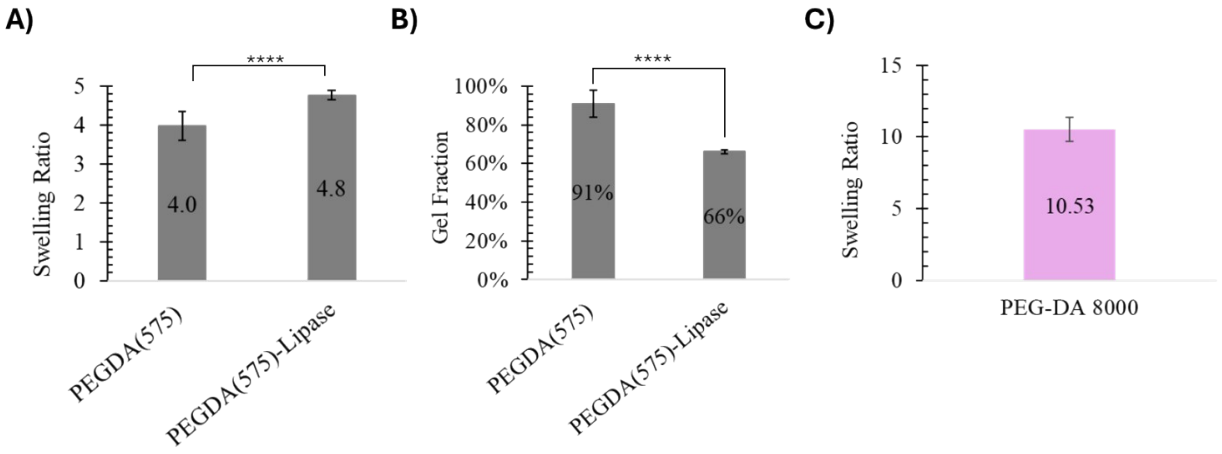

Figure S3. Swelling ratio and gel fraction of PEG-DA(575) with redox initiators A) the swelling ratio, showing a statistically significant difference in the swelling ratio between control and PEG-lipase sample (t(8), p<0.001). B) the gel fraction of control and PEG-lipase sample (t(8), p<0.001). C) Swelling ratio of PEG-DA(8000) with AAPH initiators.

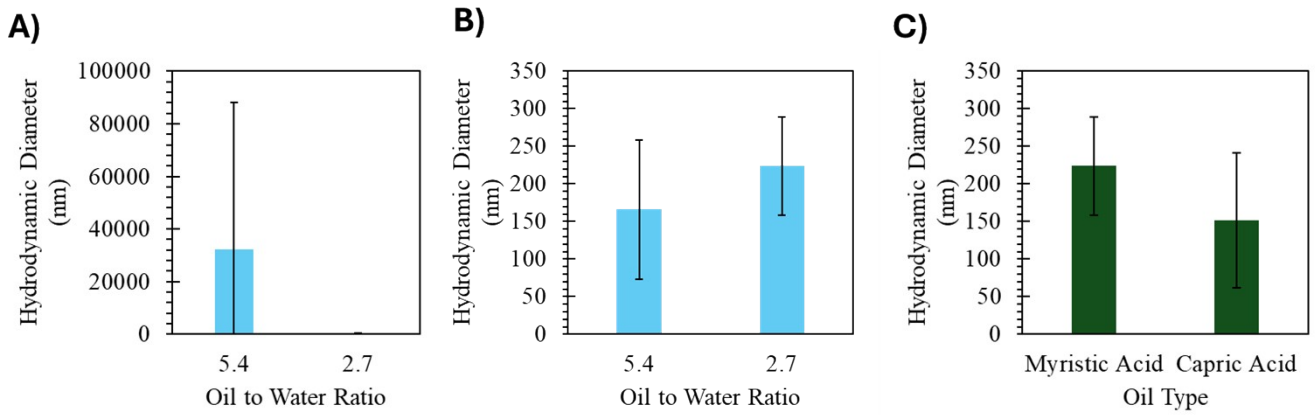

Figure S4. Hydrodynamic diameter from DLS results of syringe filtered samples pre-lyophilization A) the comparison of PEG-DA(575) with different oil-to-water ratios (n=3) B) the oil to water ratio comparison with an outlier removed (n=2 for 5.4) C) Comparison of oil type using thermal and redox polymerization.

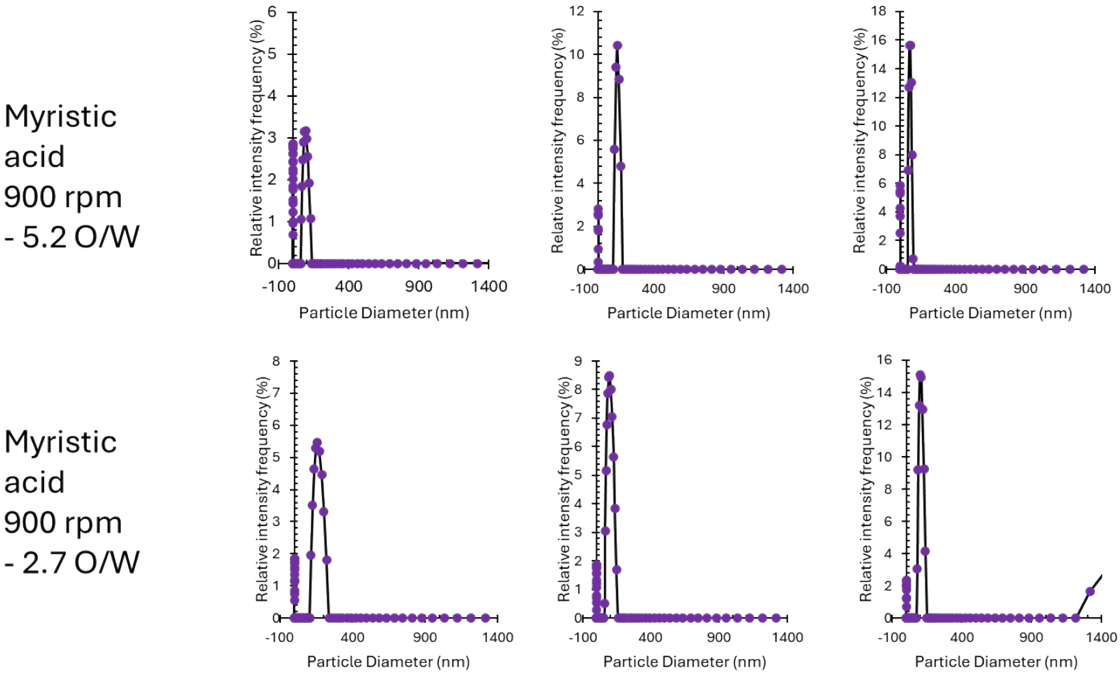

Figure S5. Particle size comparison for PEG-DA(575) nanogels stirring at 900 rpm, using temperature induced polymerization for different oil to water ratios. Each graph represents a trial and the resulting DLS post syringe filtration. The x-axis is cut off at the size of the syringe filter as nothing larger should pass through. We do see larger peaks in some samples, which are attributed to leftover oil particles growing over time.

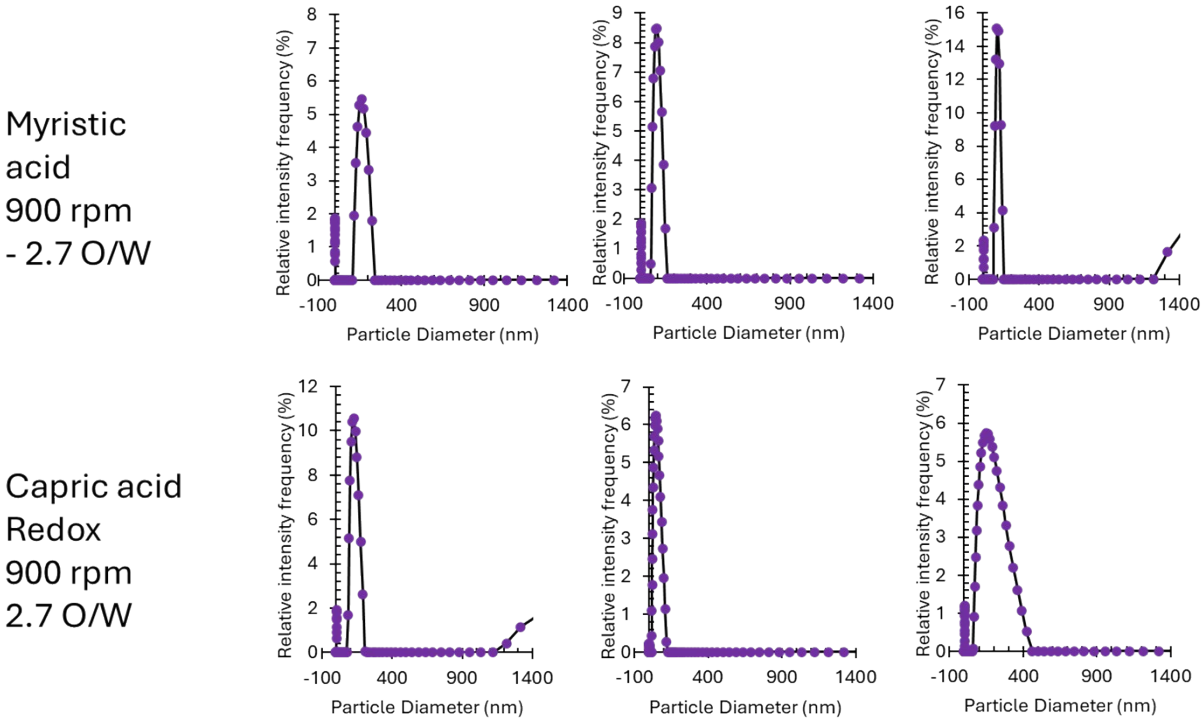

Figure S6. Particle size comparison for PEG-DA(575) nanogels stirring at 900 rpm, using temperature induced polymerization for myristic acid and using redox polymerization for capric acid. Each graph represents a trial and the resulting DLS post syringe filtration. The x-axis is cut off at the size of the syringe filter as nothing larger should pass through. We do see larger peaks in some samples, which are attributed to leftover oil particles growing over time.

,

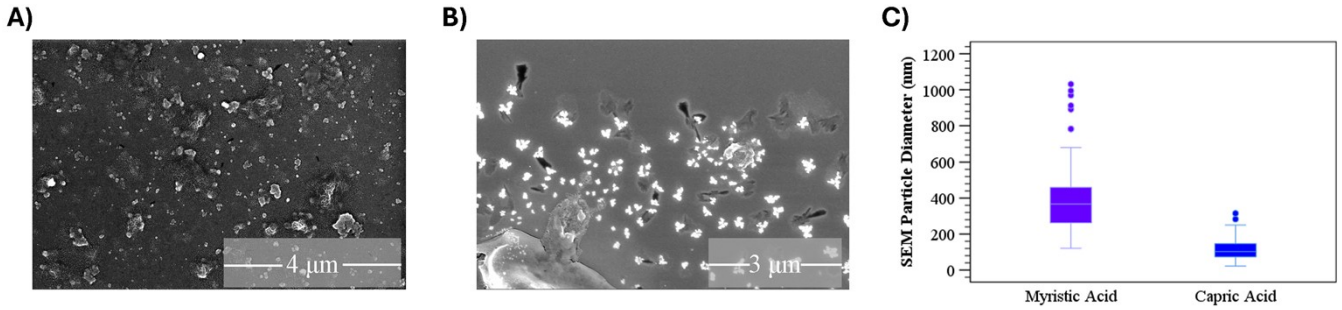

Figure S7 Comparison of thermal and redox polymerization particle size diameter using PEGDA(575) with different oils, a stirring speed of 900 rpm and oil to water ratio of 2.7:1, after lyophilization. A) SEM image of particles created using a thermal radical polymerization technique with myristic acid as the oil phase. B) SEM image of particles using redox polymerization with capric acid as the oil phase. All SEM images were at a magnification of 15,000X. C) The box plot of the SEM particle sizes analyzed with ImageJ concluded there was a larger distribution of particle sizes using the thermal system, with an average particle size of 393.55 ± 188.41 nm. The average particle size for the redox system was 78.69 ± 22.33 nm. The effect size between the two size groups was 1.45, using Cohen's *d* value and the standard deviation of the thermal system. This allows us to conclude there is a difference in the particle diameter, as the redox system resulted in effectively smaller particle size than the thermal system. (n=102, N=2 for myristic acid; n=104, N=2 for capric acid, $p<0.001$)

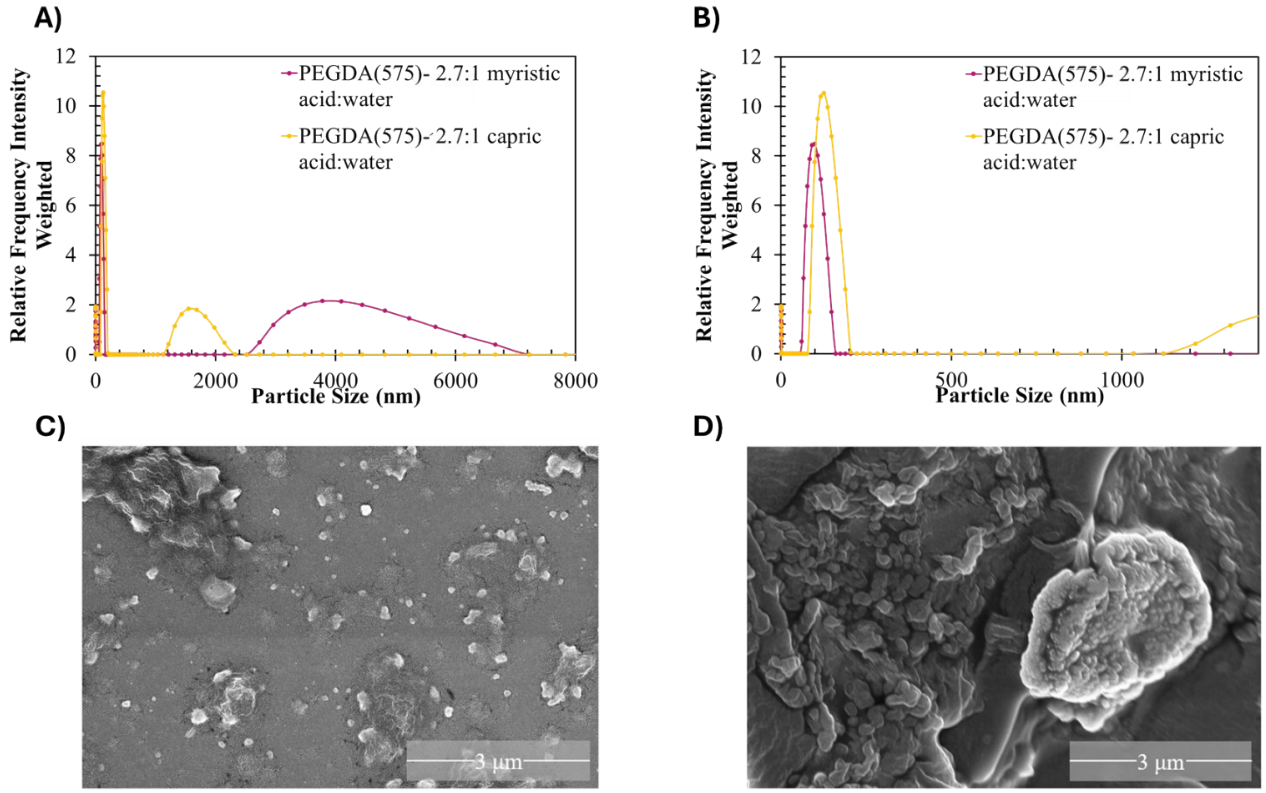

Figure S8. After an n=3 redox polymerization experiment using capric acid as the continuous phase to confirm particle formation, the particle sizes were analyzed and compared to PEG-DA(575)- 2.7:1 O/W stirring at 900 rpm immediately after syringe filtering. These samples use half the water to oil ratio as described previously. A) The DLS results for PEG-DA(575) synthesized using either capric acid (yellow) or myristic acid (magenta). The hydrodynamic diameter of the particles synthesized using capric acid was 151.5 ± 89.4 nm with a polydispersity index of 0.33 ± 0.15. Whereas, the hydrodynamic diameter for PEG-DA(575)- 2.7:1 oil to water using myristic acid 224.0 ± 65.2 nm with a PDI of 0.39 ± 0.05. For both systems, we see two peaks at larger particle sizes, that are even larger than the syringe filter. This contributed to residual oil that begins to aggregate once resuspended in water. B) The DLS plot in A) was resized to take a closer look at the size range we expected our particles to be. The peaks indicate particle sizes for the PEG-DA(575)-2.7:1 oil to water using myristic acid or capric acid were 98.74 nm and 125.90 nm, respectively. C) Represents the SEM PEG-DA(575)- 2.7:1 oil to water particles recovered from the myristic acid nanoemulsion, with the average particle size of 199.24 ± 4.42 nm (n=124, N=2). The scale is 3 µm, with a magnification of 15,000X. D) SEM image of PEG-DA(575) 2.7:1 nanogels using capric acid with the same specs for particles synthesized from the myristic acid emulsion. The average particle size was calculated to be 351.88 ± 2.18 nm.

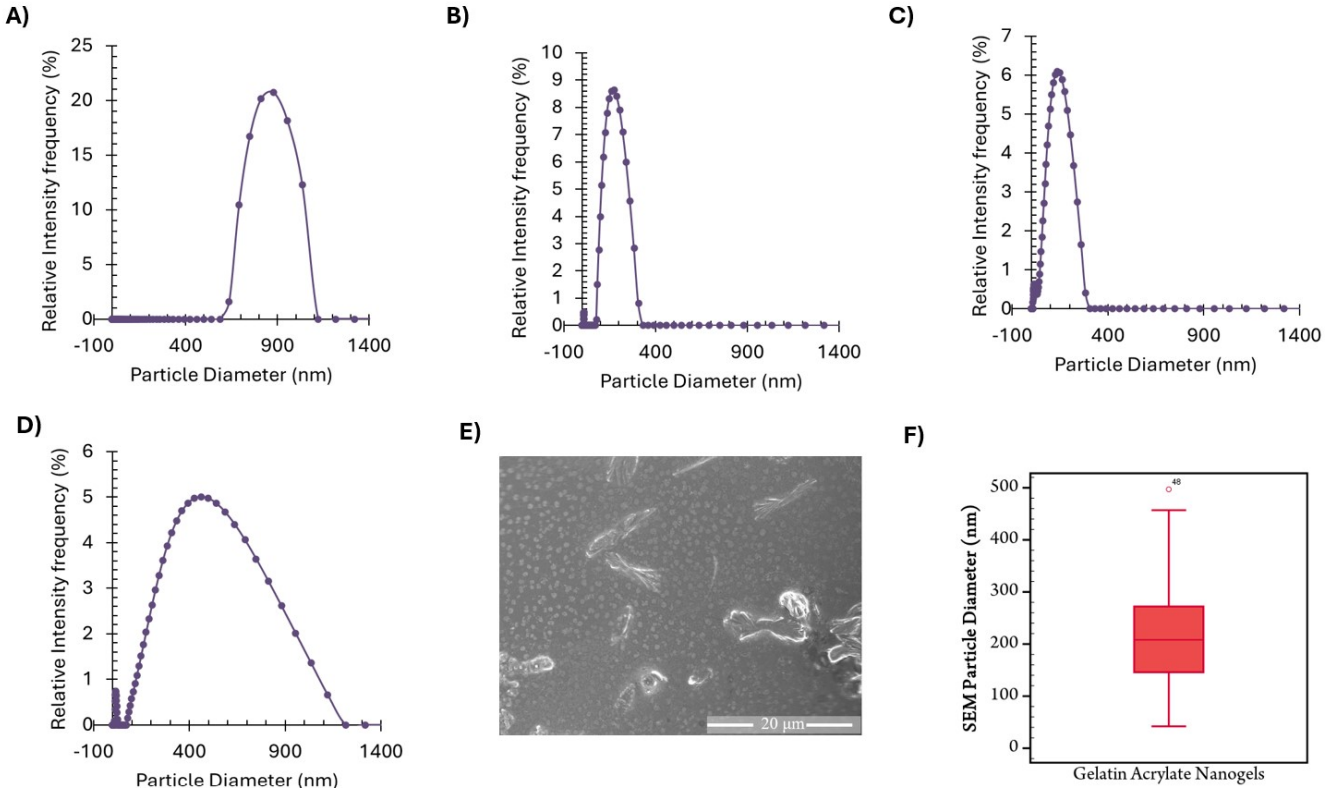

Figure S9. Gelatin acrylate nanogels synthesized using a w/o emulsion in myristic acid with solid-liquid separation. A) Particle diameter via DLS of nanogels prior to vacuum filtration. The average hydrodynamic diameter was 2015.3 nm with a PDI of 36.69%. (n=3) B) Particle diameter of nanogels post-vacuum filtration via DLS had an average particle dimeter of 2614.19 nm with a PDI of 22.58%. (n=3) C) The DLS of the nanogels post syringe filtration resulted in an average hydrodynamic diameter of 130.7 nm with a PDI of 22.55. (n=3) D) After freeze drying, the particles were resuspended in Ultra Pure Type 1 water, and the average hydrodynamic diameter of the resuspended particles was 277.1 nm with a PDI of 27.04%. (n=2). E) SEM of dried gelatin acrylate nanogels using 2404X magnification, with a scale of 20 µm. The particle diameter of the dried nanogels were analyzed using ImageJ (n=79, N=2). The average particle diameter was 204.1 ± 91.95 nm. F) Particle size distribution of

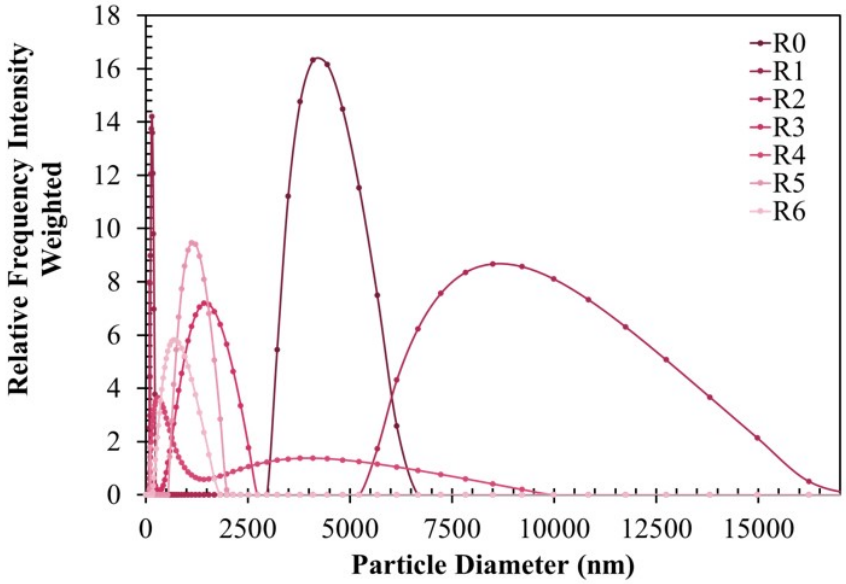

diameters calculated from SEM analysis.

Figure S10. Resuspended PEGDA(575) Trial 1 in DI water. Particles exhibited residual myristic acid, however, recycles R1, R3, R5, and R6 did not have a secondary peak as R1, R2, and R4 had. Residual myristic acid led to slight issues with SEM imaging after resuspension, requiring six washes with 15 mg/m of reagent alcohol. This concentration was experimentally calculated by finding the volume by which myristic acid is soluble. We see from our DLS results that the particle diameter

peak becomes smaller and narrower as we continue to recycle. This contributes to the increase in water in the sample, as discussed in the text.

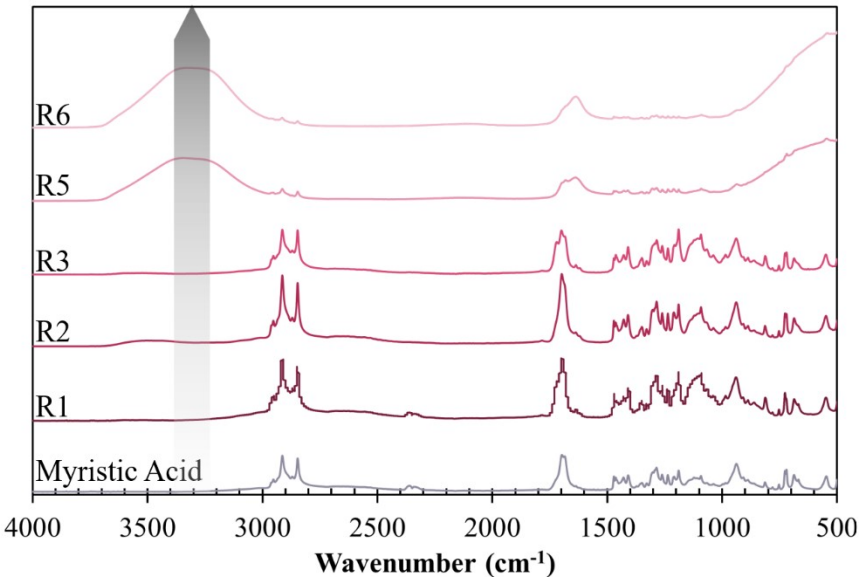

Figure S11. FTIR of pristine myristic acid and recycled myristic acid, drying for 24 hours in a fume hood at room temperature. The graph highlights an increase in water content with each subsequent oil recycling, indicated by the -OH stretching region between a wavenumber of 3000 and 3500 cm^{-1}. Water remaining in myristic acid led to a decrease in the recovery of PEG-DA(575) nanogels as our polymer is located in the water that is being suspended in myristic acid.

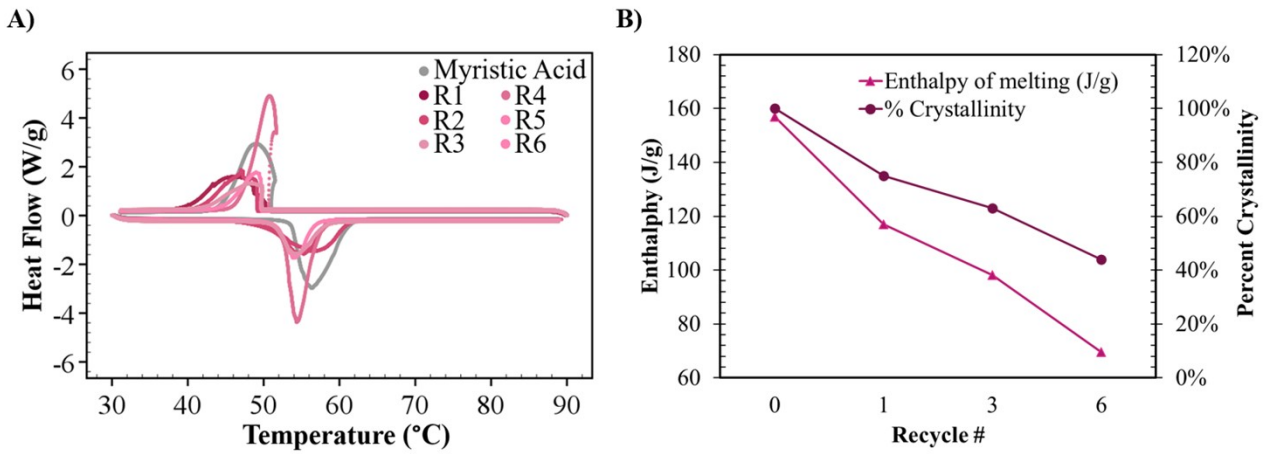

Figure S12. Evidence of the melting temperature (endothermic peak) of recovered myristic acid after recycling and allowing it to dry in the fume hood at room temperature for 24 hours. A) Provides the DSC data for both melting temperature and crystallization temperature. The melting temperature was within the range of 53.98 °C and 55.62 °C, showing minimal variability with recycling of myristic acid. Moreover, the crystallization temperature also remained within a range of 46.16 °C and 49.04 °C. B) The percent crystallinity was evaluated to determine if there were changes in the myristic acid crystallinity upon continuous recycling steps. We assumed pristine myristic acid was 100% crystalline in our calculations. There was a 77.17% decrease in percent crystallinity, pointing to a reduction in order of the crystalline state. This was determined to be associated with the water trapped within the myristic acid after recovery and vacuum filtration. As expected with a change in crystalline structure, the enthalpy of melting also decreased as we continued to recycle to oil layer.

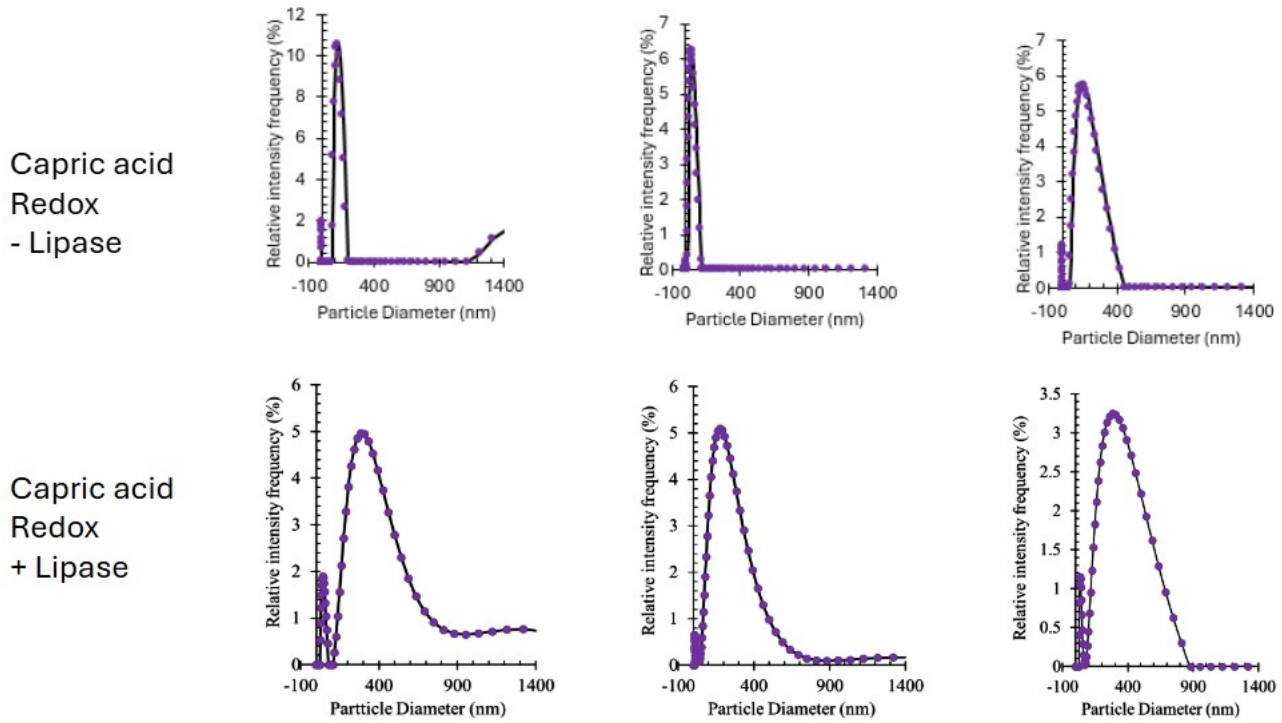

Figure S13. Particle size comparison for PEG-DA(575) nanogels stirring at 900 rpm, using redox polymerization in a nanoemulsion with capric acid as the oil layer with and without enzyme. Each graph represents a trial and the resulting DLS post syringe filtration. The x-axis is cut off at the size of the syringe filter as nothing larger should pass through. We do see larger peaks in some samples, which are attributed to leftover oil particles growing over time.

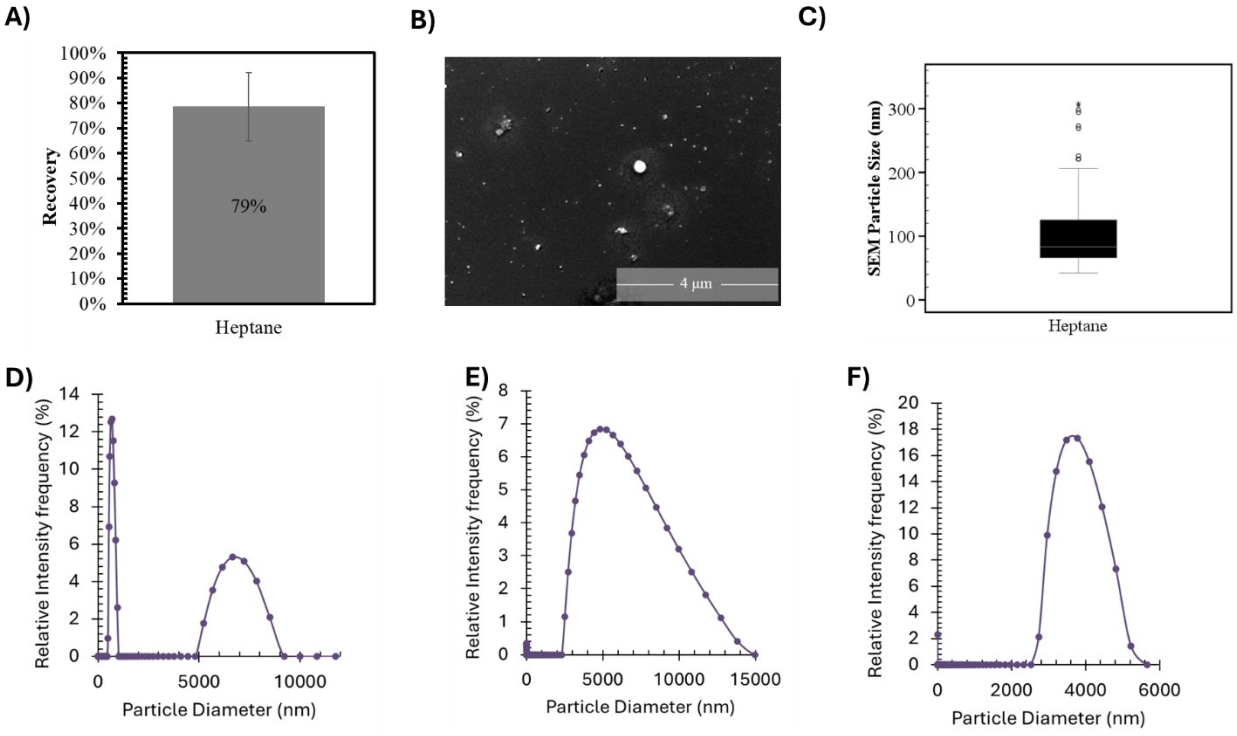

Figure S14. Comparison of A) recovery of PEG-DA(575) nanogels synthesized at 900rpm in heptane. Heptane which was run at 10 O/W which is higher than oil to water ratio utilized in the oils in the study. B) SEM image of the PEG-DA(575) nanogels synthesized in heptane. C) Particle diameters from SEM images for PEG(575) nanogels synthesized at 900rpm in heptane. The average particle size was 102.9 ± 53.24 nm (n=200, N=2) D) Resuspended heptane synthesized nanogels, trial 1. E) Resuspended heptane synthesized nanogels, trial 2. E) Resuspended heptane synthesized nanogels, trial 3.

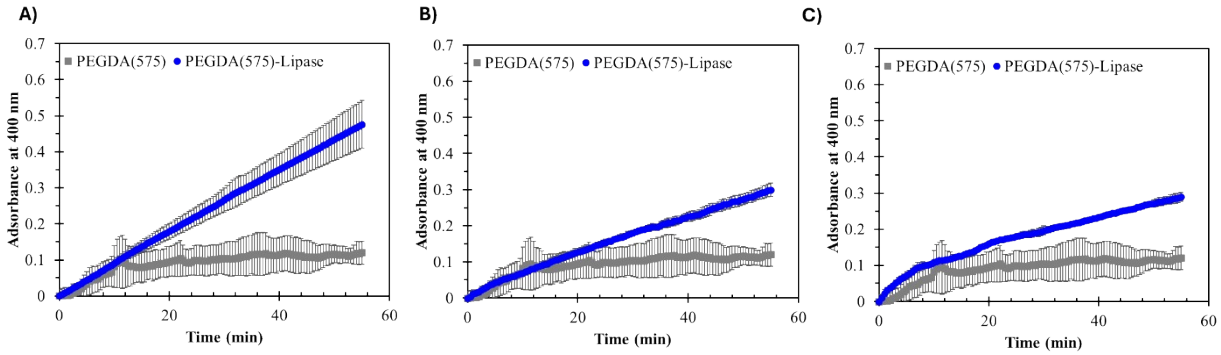

Figure S15. Enzyme kinetics assays using enzyme free and enzyme encapsulated particles. A) first trial B) second trial C) third trial

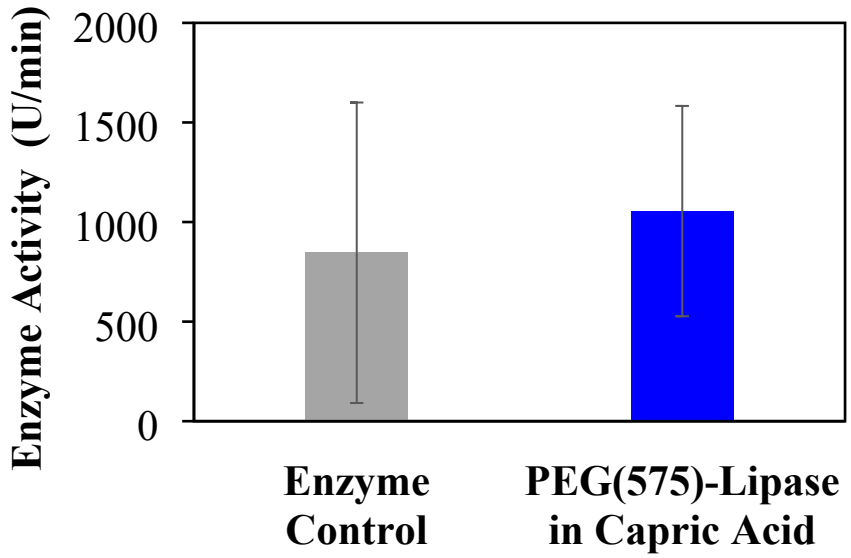

Figure S16. Enzyme activity of lipase incubated with PEG-DA(575) noted as enzyme control compared against enzyme encapsulated in particle. 1 mg of each sample was used.

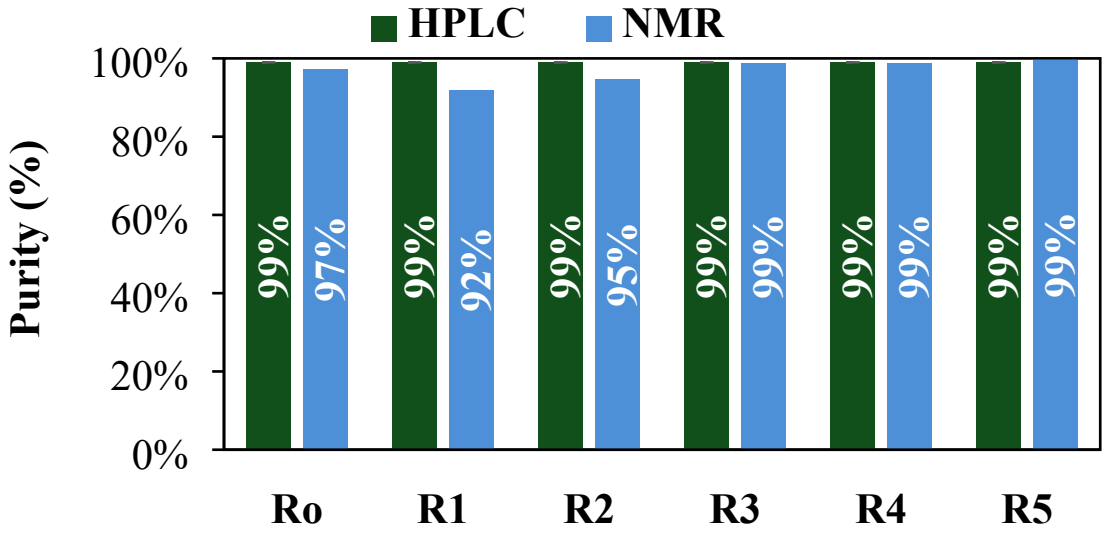

Figure S17. Purity analysis of particles obtained through myristic acid recycling studies.

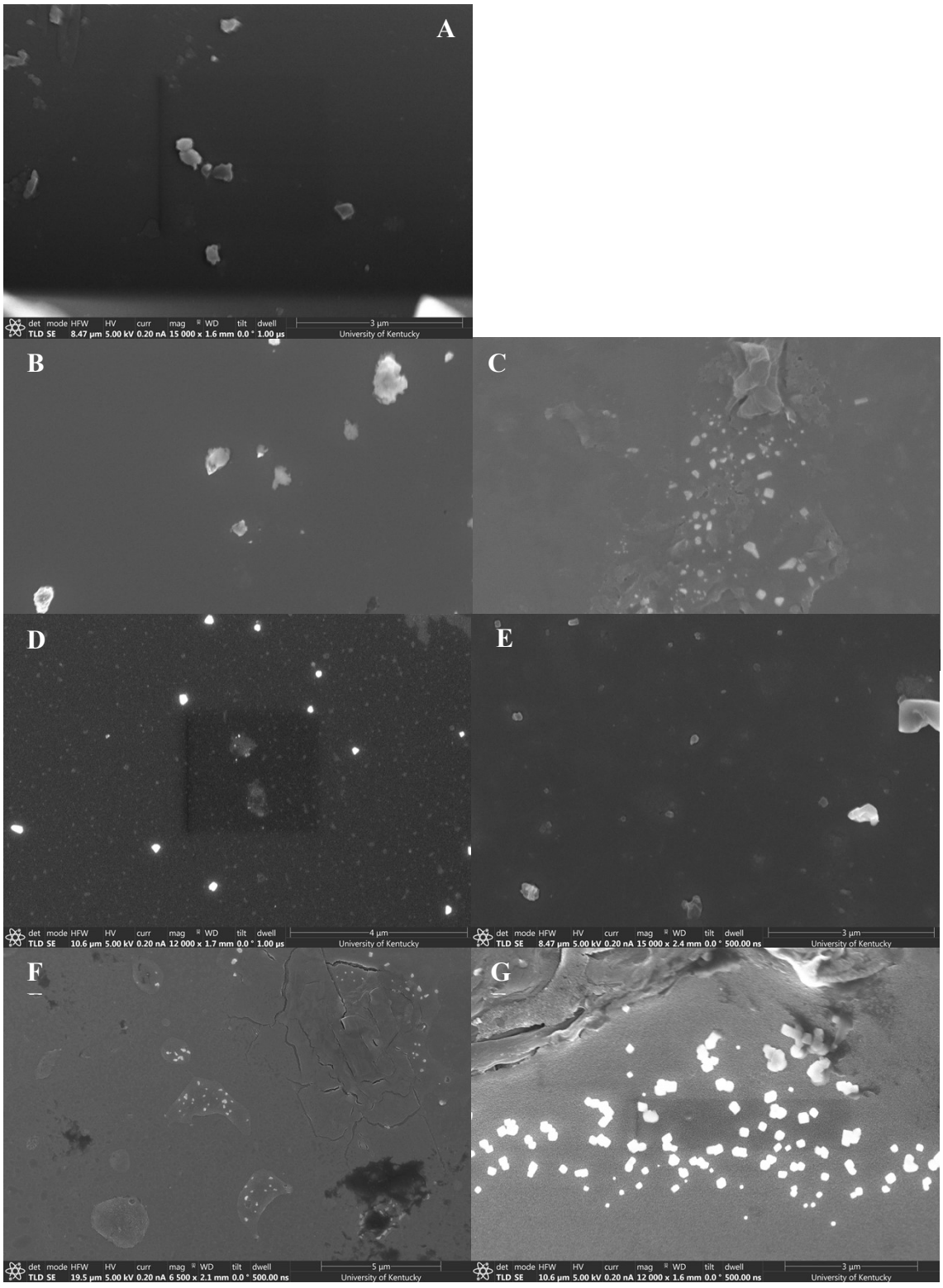

Figure S18: PEGDA(575) particles synthesized during the recycling studies using myristic acid. Some images have larger precipitates or a films which are attributed to myristic acid left over in the samples.

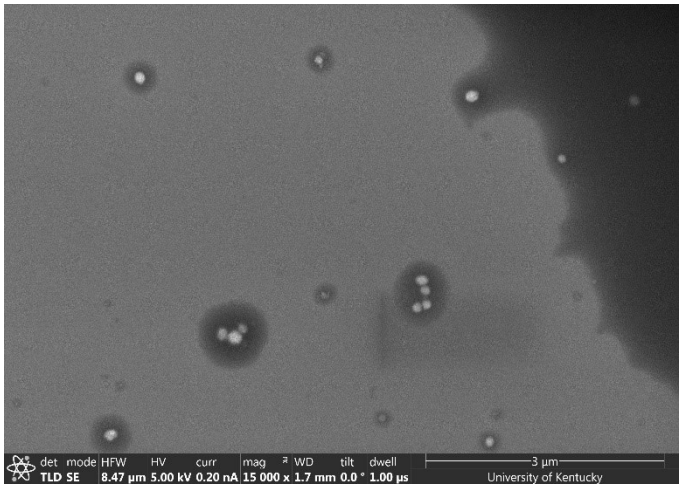

Figure S19: PEGDA(575) particles synthesized using heptane-water emulsion instead of the myristic acid or capric acid oils used in the study as a comparison.

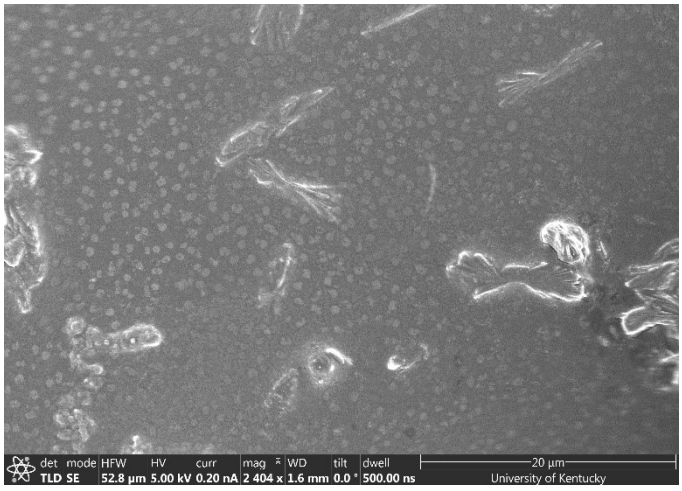

Figure S20: Gelatin particles synthesized in the work at 900rpm in myristic acid. The particles are coated with a thin layer of myristic acid due to incomplete washing of the particles prior to SEM analysis.

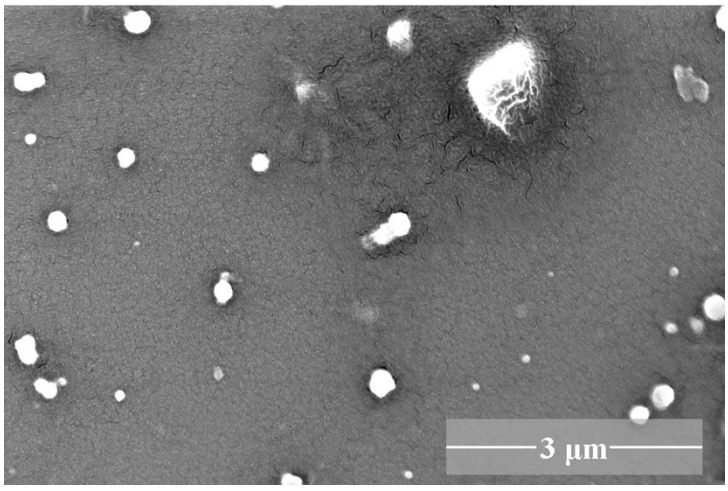

Figure S21. SEM image of PEG-DA(575) particles at 900 rpm in myristic acid.

Table S1: The summery of particle size data from the main manuscript. SEM data is determined from dried particles using ImageJ. DLS data was determined using syringe filtered solutions (within 2 hours of synthesis) prior to drying. The specific conditions of each particle synthesis can be found in the table.

Polymer	Rxn type	Oil	Water to oil ratio	Stirring (rpm)	Temp. (°C)	SEM size (nm)	DLS (nm)	DLS PDI
16.6 v/v% PEG-DA(575)	Thermal	Myristic acid	1:5.4	100	70-75	122.2 ± 22.1	139.5 ± 20.6	0.22 ± 0.04
16.6 v/v% PEG-DA(575)	Thermal	Myristic acid	1:5.4	900	70-75	310.1 ± 166.9	165.9± 92.6	0.25 ± 0.02
16.6 v/v% PEG-DA(8000)	Thermal	Myristic acid	1:5.4	100	70-75	195.8 ± 100.0	193.1 ± 87.8	0.25 ± 0.02
16.6 v/v% PEG-DA(8000)	Thermal	Myristic acid	1:5.4	900	70-75	72.1 ± 20.6	149.6 ± 83.2	0.30 ± 0.02
16.6 v/v% PEG-DA(575)	Thermal	Myristic acid	1:5.4	900	55	393.6 ± 188.4	208.1 ± 112.1	0.25 ± 0.07
16.6 v/v% PEG-DA(575)	Redox	Myristic acid	1:5.4	900	55	78.7 ± 22.3	114.8 ± 58.1	0.33 ± 0.15
15 v/v% Gelatin	Thermal	Myristic acid	1:5.4	900	70-75	204.1 ± 92.0	130.7 ± 29.8	0.23 ± 0.04
16.6 v/v% PEG-DA(575)	Redox	Capric acid	1:5.4	900	35	79 ± 22 nm	151.5 ± 89.4	0.33 ± 0.15
16.6 v/v% PEG-DA(575) w/ lipase	Redox	Capric acid	1:5.4	900	35	117.8 ± 56.9 nm	332.4 ± 126.4 nm	0.28 ± 0.06

Table S2: The summery of particle size data from the main manuscript regarding particle synthesis

during myristic acid recycling. Recycling used thermal polymerization, 100rpm, and myristic acid. SEM data is determined from dried particles using ImageJ. DLS data was determined using syringe filtered solutions (within 2 hours of synthesis) prior to drying.			
Polymer	SEM size (nm)	DLS (nm)	DLS PDI
0	122.2 ± 22.1	156.1 ± 30.6	0.22 ± 0.04
2	314.6 ± 295.6	226.3 ± 202.6	0.18 ± 0.14
4	300.9 ± 236.1	277.7 ± 138.9	0.19 ± 0.15
6	359.1 ± 205.7	101.4 ± 14.	0.28 ± 0.02

Table S3: CHEM 21 selection guide ranking of solvents and polymers involved in the study

	BP (°C)	FP (°C)	Worst H3xx [c]	H4xx	Safety Score	Health Score	Environmental Score	Ranking
Water [d]	100	na	None	None	1	1	1	Recommend
Ethanol [e]	78	13	H319	None	4	3	3	Recommend
Myristic acid [e]	326	>110	None	None	1	1	3	Recommend
Capric acid [e]	268	147	H319	H412	1	2	6	Recommend
PEG-DA	na	230	H318	None	1	4	3	Recommend
Heptane	98	-4	H304	H410	6	2	7	Problematic